GPU-ACCELERATED MODELLING OF BIOLOGICAL MEMBRANES ION-TRANSPORT

Adam Gorecki[(a,*)] , Krzysztof Dołowy[(b)]

[(a)]Warsaw University of Life Sciences WULS-SGGW, Nowoursynowska St. 159, 02-787 Warsaw, Poland
[(b)]Warsaw University of Life Sciences WULS-SGGW, Nowoursynowska St. 159, 02-787 Warsaw, Poland
[(a)]adam_gorecki@sggw.pl ,
[(b)]krzysztof_dolowy@sggw.pl
* the corresponding author

ABSTRACT

The ion-transport modeling through biological membranes is important for understanding of many life processes. The transmembrane potential and ion concentrations in the stationary state can be measured in *in-vivo* experiments. They can be also simulated within membrane models. Here we consider a basic model of ion transport that describes the time evolution of ion concentrations and potentials through a set of nonlinear ordinary differential equations.

To reduce the computation time we have developed a GPU-optimized application for simulation of the ion-flows through a membrane starting from an ensemble of initial conditions. The application is written in CUDA programming language and runs on NVIDIA TESLA family of numerical accelerators. The calculation speed can be increased over 10000 times compared with a sequential program running on a PC.

Keywords: biological membranes, electrochemistry, differential equations integration, CUDA, TESLA

1. INTRODUCTION

Every living cell has to exchange energy and mass with its environment in a selective way. An animal cell is surrounded by a lipid bilayer, called as a biological membrane (Stryer 1981). The membrane includes special proteins (channels, transporters and pumps) which enable selective transmission of ions. The activity of these transmission devices is controlled by different factors such as ion concentration, electric fields or presence of specific molecules.

Studies on ion-transport through biological membranes are crucial for understanding the etiology of many diseases. Abnormal ion transport is the cause of many serious health problems and is responsible for toxicity of many chemicals. For example, the malfunctioning of CTFR channel that controls transport of chlorine and bicarbonate ions in bronchial (lungs) epithelial tissue causes *cystic fibrosis* (Gadsby, Vergani and Csanády 2006). Problems in ion transfer through nervous cells are observed in some types of epilepsy (Scheffer and Berkovic 1997). The mechanisms of many poisons or venoms such charybdotoxin (Goldstein and Miller 1993) or iberiotoxin (Candia, Garcia and Latorre 1992**)** is based on blocking the activity of important membrane channels. A recent review of important protein channels has been presented in (Toczylowska-Maminska and Dolowy 2012).

The time evolution of membrane potentials and ion concentrations can be modeled using differential equations (Falkenberg and Jakobsson 2010, Sohma et all. 2000). The variables of the models (potentials and concentrations) can be also observed in *in-vivo* experiments. The comparison between simulations and experiments allows for optimization of model parameters to make them more realistic. In this paper we present results of simulations of transmembrane potential generated by epithelial cell monolayer. The calculations are based on phenomenological model with a reduced number of parameters.

Epithelial cells are external cells of organs contacting with external environment. An epithelial cell membrane consists of two parts:

- *basolateral* – contacting with the internal cells of the organ,
- *apical* – contacting with an external environment .

Both parts of the cell membrane are covered by a solvent which in biological system is a water solution of ions at physiological concentrations. The activity of membrane proteins and their selectivity for specific ions defines the stationary state of the system. The bilayer is polarized with membrane electric potential (so called resting potentials), which stops effective ion currents. This potential can be measured using special electrodes.

The most important ions contributing to the membrane transport are:

- potassium K+
- sodium Na+
- chlorine Cl-
- bicarbonate HCO_3-

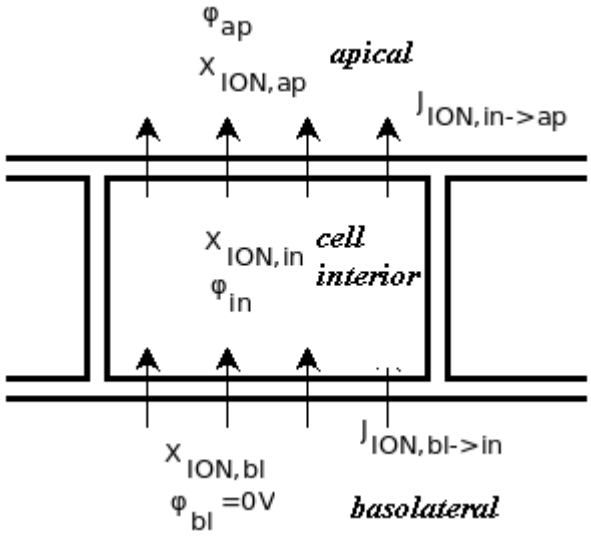

Figure 1. The considered model of ion transport in epithelial cell monolayer. The space around a cell is divided into apical(*ap*), basolateral (*bl*) and cell interior (*in*) domains

2. THE SIMULATED SYSTEM

The model of epithelial tissue considered below is illustrated on Figure 1. The cell and its neighborhood are divided into three geometrical regions: apical (*ap*), the cell interior (*in*), and basolateral (*bl*).
We assume that:

- the concentrations of ions in basolateral and apical regions are constant in time,
- the basolateral area has reference electric potential φ_{bl}=0 V.

Within our model the state of the system is fully represented by the following variables:

- the apical potential φ_{ap},
- the cell interior potential φ_{in},
- the ion concentrations in the cell interior $X_{ION,in}$, where *ION* = K+, Na+, Cl-, HCO_3-

The apical potential is equivalent to transmembrane potential because we have assumed φ_{bl}=0 V.
Potentials φ_{ap}, φ_{in} characterize the state of two capacitors created by apical and basolateral sides of the membrane. The currents charging these 'capacitors' are related to the total flows of ions of different types.

There are many models of ion flows described in literature, for example (Falkenberg and Jakobsson 2010, Sohma, Gray, Imai and Argent, 2000). These models describe time-evolution with ordinary differential equations. The equations include many parameters characterizing specific ion-channel activity. If a model contains too many parameters than usually its difficult to find their realistic values.
We proposed our model with a reduced number of parameters:

$$\partial_t \varphi_{ap} = \frac{\sum_{IONS} J_{ION}(in \to ap)}{C_{ap}} + \frac{\sum_{IONS} J_{ION}(bl \to in)}{C_{bl}}$$

$$\partial_t \varphi_{bl} = \frac{\sum_{IONS} J_{ION}(bl \to in)}{C_{bl}}$$

$$\partial_t X_{ION,in} = \frac{J_{ION}(in \to ap) - J_{ION}(bl \to in)}{F \cdot z_{ION} \cdot Vol}$$

where:

$J_{ION}(bl \to in)$ - the electric current (positive charges flow) corresponding to flow of ions type *ION* from basolateral area to the cell interior,

$J_{ION}(in \to ap)$ - the electric current (positive charges flow) corresponding to flow of ions type *ION* from basolateral area to the cell interior,

C_{bl} - the basolateral membrane capacity,

C_{ap} - the apical membrane capacity,

z_{ION} - the sign of ion type ION,

Vol - the volume of the cell,

F - the Faraday constant.

The currents of ions are given by equations:

$$J_{ION}(bl \to in) = G_{ION,bl} \cdot (-\varphi_{in} - \varphi_{Nernst}(T, z_{ION}, X_{ION,bl}, X_{ION,in})),$$

$$J_{ION}(in \to ap) = G_{ION,ap} \cdot (\varphi_{ap} - \varphi_{in} - \varphi_{Nernst}(T, z_{ION}, X_{ION,in}, X_{ION,ap})),$$

where:

$\varphi_{Nernst}(T, z_{ION}, X_{ION,src}, X_{ION,trg})$ is the Nernst equilibrium potential for *ION* and flow direction of *src* → *trg*,

$G_{ION,ap}$, $G_{ION,bl}$ are effective electric permeabilities (reciprocal resistance) of apical and basolaterar side of membrane, respectively.

The Nernst resting potential (Wright 2004) is defined as

$$\varphi_{Nernst}(T, z_{ION}, X_{ION,src}, X_{ION,trg}) =$$

$$= -\frac{RT}{Fz_{ION}} \cdot \ln\left(\frac{X_{ION,src}}{X_{ION,trg}}\right),$$

where T is absolute temperature of solvent.
When the potential difference between the sides of membrane *src*, *trg* is equal to Nernst potential, there is no effective current of ion of type *ION*.

3. IMPLEMENTATION

The simulation program is written in CUDA C language and designed to work on NVIDIA TESLA family graphical accelerators (NVIDIA company 2012).

The general idea of our approach is to perform the same operations on different data in parallel – it is so called Single Instruction Multiple Data approach. For our applications (the same algorithm, many data sets, small amount of required operational memory) we need many instances of simple scalar calculations. NVIDIA GPU accelerator is perfectly suited for such task, because we can perform separate simulations on different cores. We expect the maximum speedup if the number of separate tasks does not exceed the maximum number of threads allowed to run in parallel. In our application the GPU accelerator works as a computer farm executing separate instances of the same program, so we have not used advanced CUDA environment features, such as dedicated numerical libraries or texture processing.

To integrate the differential equations we use the forth-order Runge-Kutta integration scheme.
The host process creates GPU device processes performing simulations starting from different initial conditions (for example ion concentrations) or different membrane parameters (see Figure 2). This approach can give linear speedup as a result of parallel calculations on separate threads with no shared memory.

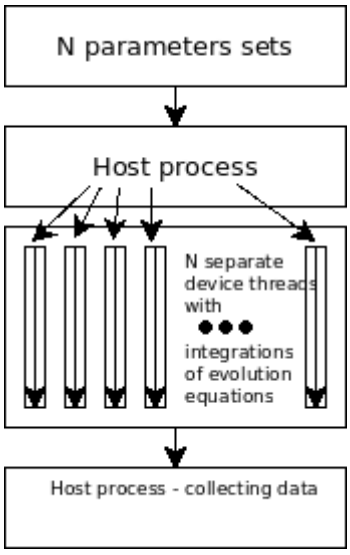

Figure 2. GPU optimization of N instances of simulations of the system. The host process reads initial data and parameters, distributes these sets in GPU device memory, and launches apropriate number of GPU device threads. Each GPU thread performs simulation for one parameters set.

The host process collects the data. Usually we do not need the whole evolution of the system, but only the values of variables when the system has converged to the stationary state.

4. RESULTS

The example results illustrating transmembrane potential φ_{ap} are shown on Figure 3-6.

The contour plots show transmembrane potential value in volts[V] as a function of two variables: concentrations of potassium K+ and sodium Na+ ions at apical side of the cell. The ion concentrations is given in milimoles per litre [mM].

The concentrations of other ions in other areas, the membrane permeabilities $G_{ION,ap}$, $G_{ION,bl}$, membrane capacities C_{bl}, C_{ap}, and the temperature T are the same for all calculations.

The parameters used in simulations are given in Table 1.

The calculations of transmembrane potential were performed for a grid of 9 x 15 = 135 parameter sets with:

- K+ ion concentation $X_{K+,ap}$changing from 1 mM to 9 mM with step 1 mM,
- Na+ ion concentration $X_{Na+,ap}$ changing from 40 mM to 180 mM with step 10 mM.

The average time of calculations on NVIDIA TESLA C870 graphics accelerator was about **0.175 seconds** of total time, comparing to about **40 minutes** in for a scalar calculations using program compiled by Free Pascal Compiler on AMD Athlon 2 GHz.

So we have a speedup **greater than 10000 !**
Such speedup it is probably related to very good computational performance and communication with local memory of NVIDIA GPU cores compared to conventional CPU.

Figure 3 shows the stationary value of the transmembrane potential for the normal membrane conductivity for all ions. As we can see, the relationship between the potential and K+, Na+ concentrations is strongly nonlinear. Small differences in K+ ion concentrations have an important influence on the potential. The transmembrane potential function $\varphi_{ap}(X_{K+,ap}, X_{Na+,ap})$ does not factorize as a product of two functions depending on single ion concentrations.

Figure 4 shows the stationary value of the transmembrane potential when K+ ion transport is block at the apical side of a membrane. As we can expect, the membrane potential depends of Na+ concentrations only. The values of transmembrane potential are different than in the normal case described previously because the calculation starts from different initial membrane potential φ_{ap} . We assumed that membrane capacities were not charged before evolution started.

Figure 5 shows the stationary value of the transmembrane potential for the normal membrane

conductivity for all ions as a function of Na+ and Cl- concentrations. The same potential as a function of concentration of HCO_3- and Cl- ions is illustrated in Figure 6. As we can see, the contribution of those ions for transmembrane potential is less significant than the influence of potassium ion.

CONCLUSIONS

We have developed a tool for modeling membrane ion flows working on NVIDIA graphics accelerators. The program increases the speed of calculations over 10000 times if compared with a our previous approach running on a scalar CPU.

Our GPU program may be very useful for membrane model parameterization and its experimental verification. Thanks to its speed we can optimize model parameters like membrane permabilities and capacities using a large number of experimental data. Moreover the code can be easily modified to other forms of differentials equations.

The model reported above threats the membrane as a single entity without focusing on particular ion channels. It can be easily generalized for a specific type membrane by modification of $J_{ION}(src \to trg)$ terms. We can consider different current-voltage characteristics of specific protein channels by selecting an appropriate $J_{ION}(src \to trg)$ term form.

The speed achieved on GPU accelerators seems to be sufficient for non-local model of membrane transport. In such models channels of different types are spatially distributed on the membranes and the equilibration process involves local currents flowing inside the cell.

In future we also plan to develop a user-friendly graphical interface, which will make the program simpler for scientist and students who are not computational experts.

ACKNOWLEDGMENTS

The work was supported by Ministry of Science and Higher Education Grant No 1828/B/PO1/2010/39.

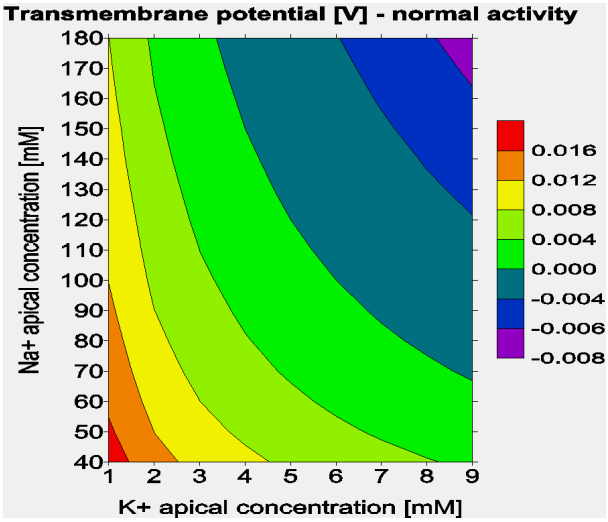

Figure 3. Example results from membrane flows simulation . The transmembrane potential (potential between basolateral side and apical side) as a function of variables - concentrations of K+ and Na+ ions at apical side. The normal transport of all ions is assumed.

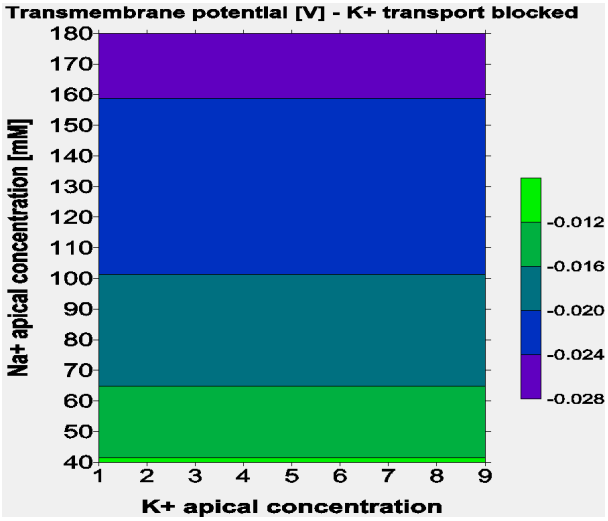

Figure 4. As Figure 3, but for the blocked transport of K+ ions.

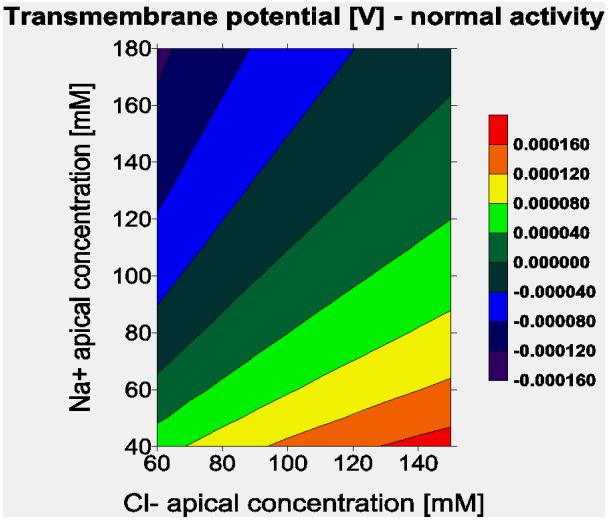

Figure 5. The transmembrane potential as a function of Na+ and Cl- apical concentrations. K+ and HCO_3- concentrations remains constant and equal to $X_{K+,ap}$ =5mM, $X_{HCO3-,ap}$ =24 mM respectively.

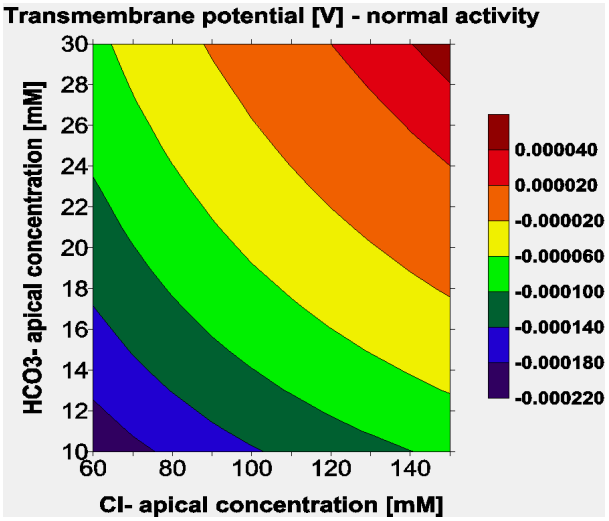

Figure 6. The transmembrane potential as a function of HCO3- and Cl- apical concentrations. K+ and Na+ concentrations remains constant and equal to $X_{K+,ap}$ =5mM, $X_{Na-,ap}$ =140 mM respectively.

Table 1: Membrane flow model parameters used for example results

Parameter	Value	Unit
Ion concentrations at apical side		
$X_{K+,ap}$	1-9, step 1	mM
$X_{Na+,ap}$	40-180, step 10	mM
$X_{Cl-,ap}$	110	mM
$X_{HCO3-,ap}$	24	mM
Ion concentrations at basolateral side		
$X_{K+,bl}$	5	mM
$X_{Na+,bl}$	120	mM
$X_{Cl-,bl}$	110	mM
$X_{HCO3-,bl}$	24	mM
Temperature		
T	300	K
Apical side permeability (reciprocal resistance)		
$G_{K+,ap}$ - Figure 3	$5 \cdot 10^{-4}$	Ω^{-1}
$G_{K+,ap}$ - Figure 4	0	Ω^{-1}
$G_{Na+,ap}$	$5 \cdot 10^{-4}$	Ω^{-1}
$G_{Cl-,ap}$	$5 \cdot 10^{-4}$	Ω^{-1}
$G_{HCO3-,ap}$	$5 \cdot 10^{-4}$	Ω^{-1}
Basolateral side permeability (reciprocal resistance)		
$G_{K+,bl}$	$5 \cdot 10^{-3}$	Ω^{-1}
$G_{Na+,bl}$	$5 \cdot 10^{-3}$	Ω^{-1}
$G_{Cl-,bl}$	$5 \cdot 10^{-3}$	Ω^{-1}
$G_{HCO3-,bl}$	$5 \cdot 10^{-3}$	Ω^{-1}
Apical side capacity		
C_{ap}	10^{-6}	F
Basolateral side capacity		
C_{bl}	10^{-5}	F
Cell volume		
Vol	10^{-9}	m^3

REFERENCES

Toczylowska-Maminska, R., Dolowy, K., 2012.
Ion transporting proteins of human bronchial epithelium.
Journal of Cellular Biochemistry 113:426-432.

Stryer, L., 1981.
Biochemistry, New York: W. H. Freeman,

NVIDIA corporation, 2012.
CUDA C Programming Guide
Available from:
http://developer.NVIDIA.com/NVIDIA-gpu-computing-documentation
Accesed: Jul 11, 2012

Falkenberg, C. V. , Jakobsson, E., 2010.
A Biophysical Model for Integration of Electrical, Osmotic, and pH Regulation in the Human Bronchial Epithelium.
Biophysical Journal 98:1476–1485.

Sohma, Y., Gray, M.A., Imai, Y. , Argent, B.E., 2000.
HCO_3^- Transport in a Mathematical Model of the Pancreatic Ductal Epithelium
Journal of Membrane Biology 176:77–100.

Gadsby, D.C., Vergani, P., Csanády, L., 2006.
The ABC protein turned chloride channel whose failure causes cystic fibrosis.
Nature 7083: 477–83.

Scheffer, I., Berkovic, S., 1997.
Generalized epilepsy with febrile seizures plus. A genetic disorder with heterogeneous clinical phenotypes.
Brain 120: 479–90.

Goldstein, S.A., Miller, C., 1993.
Mechanism of charybdotoxin block of a voltage gated K+ channel.
Biophysical Journal 65:1613–1619.

Candia, S., Garcia, M.L., Latorre, R., 1992.
Mode of action of iberiotoxin, a potent blocker of the large conductance Ca(2+)-activated K+ channel.
Biophysical Journal 63:583–590.

Wright, S.H., 2004.
Generation of resting membrane potential.
Advances in Physiology Education 28:139-142.